nature climate change

Article

https://doi.org/10.1038/s41558-022-01490-7

Climate-mediated shifts in temperature fluctuations promote extinction risk

Received: 2 March 2022

Accepted: 31 August 2022

Published online: 20 October 2022

Check for updates

Kate Duffy[1,2,3] ✉, Tarik C. Gouhier[4] and Auroop R. Ganguly[1,5]

Climate-mediated changes in thermal stress can destabilize animal populations and promote extinction risk. However, risk assessments often focus on changes in mean temperatures and thus ignore the role of temporal variability or structure. Using Earth System Model projections, we show that significant regional differences in the statistical distribution of temperature will emerge over time and give rise to shifts in the mean, variability and persistence of thermal stress. Integrating these trends into mathematical models that simulate the dynamical and cumulative effects of thermal stress on the performance of 38 globally distributed ectotherm species revealed complex regional changes in population stability over the twenty-first century, with temperate species facing higher risk. Yet despite their idiosyncratic effects on stability, projected temperatures universally increased extinction risk. Overall, these results show that the effects of climate change may be more extensive than previously predicted on the basis of the statistical relationship between biological performance and average temperature.

Biodiversity loss has been recognized as one of the top global risks by the World Economic Forum because it could erode or eliminate key ecosystem functions and services[1]. Climate change is expected to surpass habitat loss as the leading threat to global biodiversity by the middle of the twenty-first century[2]. Observed changes in the distribution and phenology of species have already been linked to climate fluctuations in numerous studies[3]. Although conservation actions may ameliorate potential biodiversity loss, the success of these efforts depends on our ability to predict the response of ecological systems to environmental changes.

Most ecological impact studies so far have relied on statistical models, such as bioclimate envelope approaches, to determine how climate change will impact ecological populations[4–7]. Bioclimate envelope models are typically constructed by either mapping the geographical distribution of species to co-located temperature records via regression techniques or by building species' thermal profiles via empirical assessments of their performance across a range of temperatures (that is, thermal performance curves or TPCs)[4,8]. These relationships between organisms and temperature are then used to predict the distribution of species under future thermal conditions projected under various climate change scenarios.

Despite the power and popularity of TPCs, these statistical approaches can yield inaccurate predictions because they typically rely on mean annual conditions and thus ignore the influence of the temporal structure of temperature fluctuations at finer scales. This is problematic because the nonlinear relationship between temperature and most metrics of biological performance essentially guarantees that the average organismal response will not be equivalent to their response to the average condition[9–12]. Specifically, when an organism is exposed to a sequence of temperatures x, its performance at the average temperature $f(\bar{x})$ will differ from the average of its performance $\overline{f(x)}$. Temporal variation in temperature will either magnify $\left(\overline{f(x)} > f(\bar{x})\right)$ or dampen $\left(\overline{f(x)} < f(\bar{x})\right)$ the effects of its mean on organismal performance depending on the curvature of f (that is, whether f is accelerating or decelerating[9]). In many cases, changes in temperature variability can be as or more important than changes in the mean value[13,14]. In one study,

[1]Sustainability and Data Sciences Laboratory, Department of Civil and Environmental Engineering, Northeastern University, Boston, MA, USA. [2]NASA Ames Research Center, Moffett Field, CA, USA. [3]Bay Area Environmental Research Institute, Moffett Field, CA, USA. [4]Department of Marine and Environmental Sciences, Marine Science Center, Northeastern University, Nahant, MA, USA. [5]Pacific Northwest National Laboratory, Richland, WA, USA. ✉e-mail: duffy.m.kate@gmail.com

climate-mediated changes in mean temperature alone were found to broadly promote organismal performance in ectotherms, but accounting for the temporal variability of temperature dampened this effect and led to most species suffering a performance loss[15].

Although the temporal structure of temperature can theoretically be incorporated into bioclimate envelope models by using finer temporal scale data, accounting for its dynamical effects on organisms is much more difficult because of the 'static' nature of these methods and their general inability to account for the cumulative effects of previous temperatures on organismal performance. However, theory has shown that such carryover effects associated with the temporal structure or autocorrelation of temperature can interact with the magnitude of temperature variability to determine population persistence[16]. Specifically, temporally autocorrelated variation tends to reduce extinction risk by decreasing the likelihood of catastrophic conditions under strong variation, whereas temporally autocorrelated variation tends to promote extinction risk under weak variation by increasing the likelihood that organisms will experience long stretches of poor conditions[16]. Prolonged exposure to temperatures above the species' critical thermal maximum is particularly destabilizing as it can reduce population fitness below the replacement rate[17]. Analyses of historical observations and projections from previous generation climate models have found strong temporal trends in the variability and autocorrelation of temperature[18–21], suggesting the potential for a larger impact on ecological populations in the future. Overall, these empirical and theoretical results highlight the importance of quantifying changes in the mean, variability and autocorrelation of temperature projected under climate change to predict their joint influence on ecological systems over the course of the twenty-first century. However, disparities in the scale of models in climate and ecology have hindered impact studies that consider the complexity of both underlying systems[22,23].

We briefly illustrate the potential for complex interactions between climate-mediated changes in the mean, variability and autocorrelation of temperature to influence organismal performance by simulating the effects of synthetic temperature time series on the population growth rate r according to a species' TPC (Fig. 1, see Methods for modelling details). Predictably, performance under negligible temperature variation can be inferred directly from the mean of each species' TPC (Fig. 1b,c). However, when temporal variation in temperature is included in the model (that is, standard deviation; shaded region), time-averaged performance can be considerably modified[9], even overturning the identity of 'winning' and 'losing' species based solely on constant temperature conditions (Fig. 1d,e). Temperature autocorrelation, which measures the temporal structure of temperature fluctuations (for example, the persistence of extremes), can also play a pivotal role in determining whether a species' performance and stability will benefit or suffer under different thermal regimes (Fig. 1f,g). To determine the impact of such changes over the course of the twenty-first century, we analysed the latest generation of Earth System Models from the Coupled Model Intercomparison Project Phase 6 (CMIP6) to document spatiotemporal changes in three key aspects of air temperature: statistical distribution, variance and temporal autocorrelation. We then analysed the effects on population stability and extinction risk using simple mathematical models to examine the hypothesis that even under ideal conditions, popular statistical methods can yield incorrect predictions about patterns of organismal performance when dynamical and cumulative temperature effects are ignored.

Regional trends in temperature distribution

We examined changes in the global and regional temperature distributions at each geographical location between 1850 and 2100 under the high emissions scenario, SSP5-8.5[24] (Fig. 2a,b). Quantile regression was used to measure temporal trends in the entire distribution of projected temperatures (that is, across quantiles ranging from $\tau = 2.5\%$ at the low end to $\tau = 97.5\%$ at the high end) in the Northern Hemisphere Extra-tropics (NHEX, 30° N to 90° N), the Southern Hemisphere Extra-tropics (SHEX, 90° S to 30° S), and the Tropics (TROP, 30° S to 30° N). When averaging trends across regions, we found asymmetrical but uniformly positive trends across all quantiles, indicating that the entire temperature distribution is shifting upwards but at rates that vary systematically across the distribution. In NHEX, the lowest quantile of the distribution ($\tau = 2.5\%$, 0.33 K per decade) is warming at twice the rate of the uppermost quantile ($\tau = 97.5\%$, 0.16 K per decade). The SHEX exhibits a similar pattern of disproportionate warming for the low quantiles ($\tau = 2.5\%$, 0.15 K per decade; $\tau = 97.5\%$, 0.10 K per decade). Conversely, in the tropics, the upper quantiles of temperature are warming faster ($\tau = 97.5\%$, 0.14 K per decade) than the lower quantiles ($\tau = 2.5\%$, 0.10 K per decade). The magnitude of trends is greater in NHEX than in SHEX or TROP. The more pronounced extra-tropical decrease in the incidence of cold events may benefit cold-limited species; however, quantile trends also indicate increased positive skewness of the NHEX temperature distribution, which has been associated with declines in long-term ecological performance[15]. Across all eight CMIP6 models that we analysed and in all three latitudinal regions, trends in the tails of the distributions differ from the trends in the central tendencies, thus highlighting the importance of moving beyond mean temperature when predicting organismal performance.

Trends in the variability of temperature between 1850 and 2100 are predicted to exhibit similarly complex regional patterns (Fig. 2c). Variance will generally increase across temperate and tropical land areas below 45° N, with regional exceptions including Asia. The strongest increases in variance are in the northern mid latitudes, including northern Africa, southern Europe, the Middle East and the western United States. Variance is decreasing most rapidly in the high northern latitudes, especially in Canada and Russia[25]. The concurrent decrease in variability at high latitudes and its increase at other latitudes suggests that temperature variation, similar to mean temperature, is becoming more spatially homogeneous in a warming world. These findings are generally consistent with studies of the previous generation of climate models, which suggested increasing temperature variability in tropical countries[26] and decreasing variability in the northern mid to high latitudes[27]. Trends at the regional level are congruent with quantile trends (Fig. 2a), which indicate a widening temperature distribution (increasing variance) in TROP, and a narrowing temperature distribution (decreasing variance) in NHEX and SHEX, as well as large-scale changes in physical climate processes[26–28]. The effects of these trends in temperature variation on ecological systems will depend on the geographical location and physiological properties of each species, with increasing variability either promoting or reducing performance on the basis of its position relative to the inflection point of an organism's TPC[9].

Frequency-resolved temperature changes

To better understand these spatiotemporal patterns, we used time-frequency decomposition via the wavelet transform to resolve changes in the variability of temperature at sub-annual to annual timescales (between 2 d and 2 yr) and multi-annual timescales (between 2 yr and 30 yr; Extended Data Fig. 1). Wavelet transforms resolve a signal in both the time and frequency domains to describe how each frequency or period in the time series contributes to variation over time. We found countervailing trends in scale-specific variability in the mid to high northern latitudes. The magnitude of short-term variability is decreasing, while the magnitude of long-term variability is increasing. Arctic amplification, which is detectable in both observational data and climate simulations, has previously been suggested as the main driver of decreasing sub-seasonal variability at these latitudes[27]. Meanwhile at the mid latitudes, variation in both annual and multi-annual timescales is increasing, consistent with increasing variance at all periodicities. These scale-dependent changes in the temporal trends of temperature fluctuations could have important ecological implications because the

https://doi.org/10.1038/s41558-022-01490-7

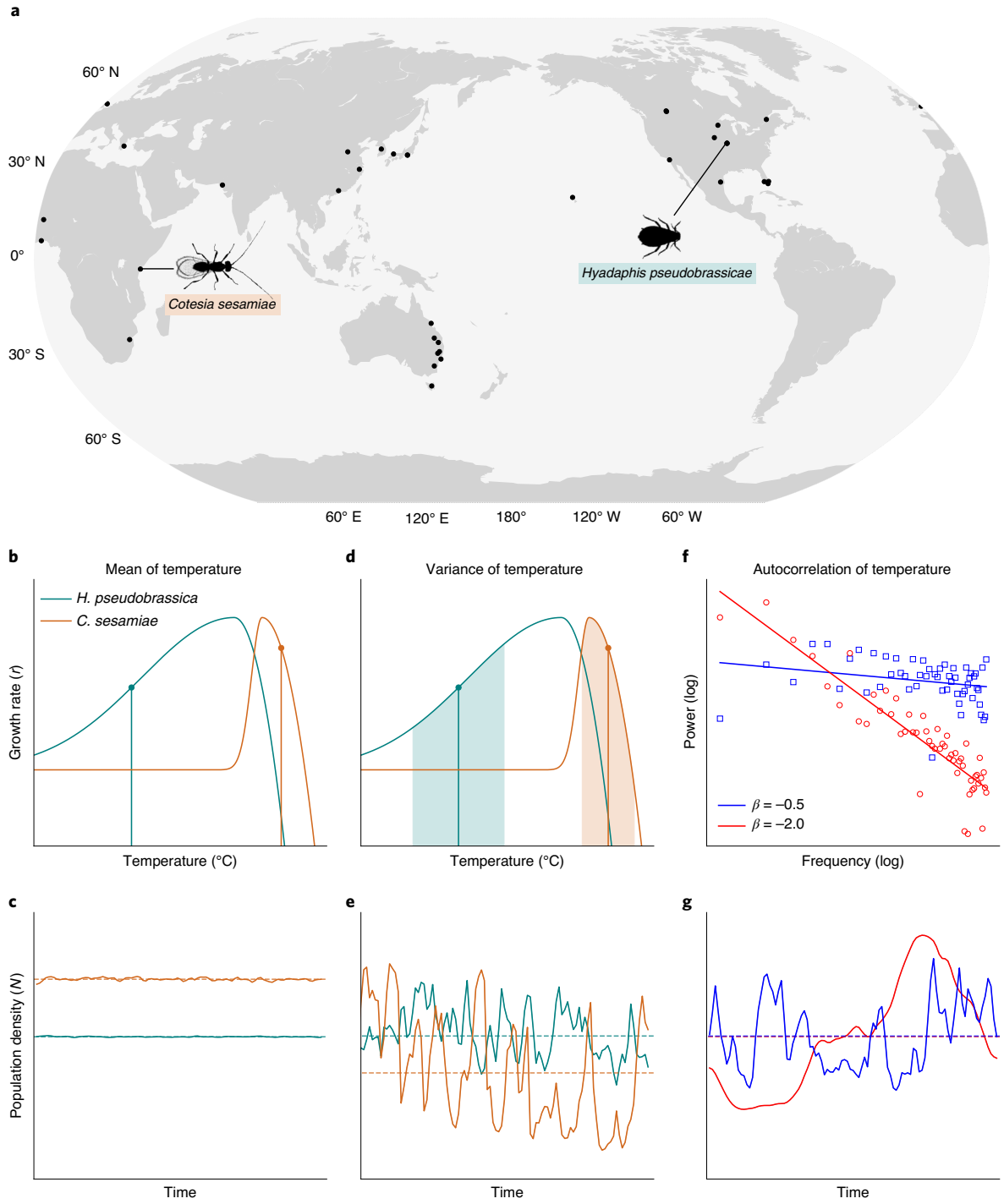

Fig. 1 | Effects of temperature mean, variance and autocorrelation on organismal performance. a, Source locations of the 38 species whose thermal performance parameters were obtained from the Deutsch et al.[5] dataset. *Cotesia sesamiae* is a tropical parasitoid wasp and *Hyadaphis pseudobrassicae* is a temperate-zone turnip aphid. **b**,**c**, Thermal performance curves and population dynamics for *C. sesamiae* and *H. pseudobrassicae* under a mean temperature (vertical line) with negligible variation. **d**,**e**, Larger temperature variation (s.d., shaded) alters mean response (dashed horizontal line) and may even overturn predictions of relative performance based on constant temperature conditions. **f**, The power spectrum of temperature with weak ($\beta = -0.5$) and strong ($\beta = -2$) temporal autocorrelation. **g**, Population dynamics of *Hyadaphis pseudobrassicae* under a greater degree of temporal autocorrelation exhibit longer-term fluctuations. Multiple aspects of temperature, such as its mean and variance, can interact to promote or decrease performance.

effect of temperature fluctuations depends on the relationship between their period and the generation time of organisms. Indeed, estimating the biological effect of temperature fluctuations by 'nonlinear averaging' of organismal performance under the relevant constant thermal regimes is much more likely to yield accurate results when the period of the temperature fluctuations is larger than the generation time of an organism because such slow variation can more easily be 'tracked' by a population[29].

We computed the spectral exponent of the temperature time series at each geographical location to quantify spatiotemporal trends, with more negative exponents indicating greater temporal autocorrelation over a range of lags from 2 d to 10 yr (Fig. 3a). We found increasing

https://doi.org/10.1038/s41558-022-01490-7

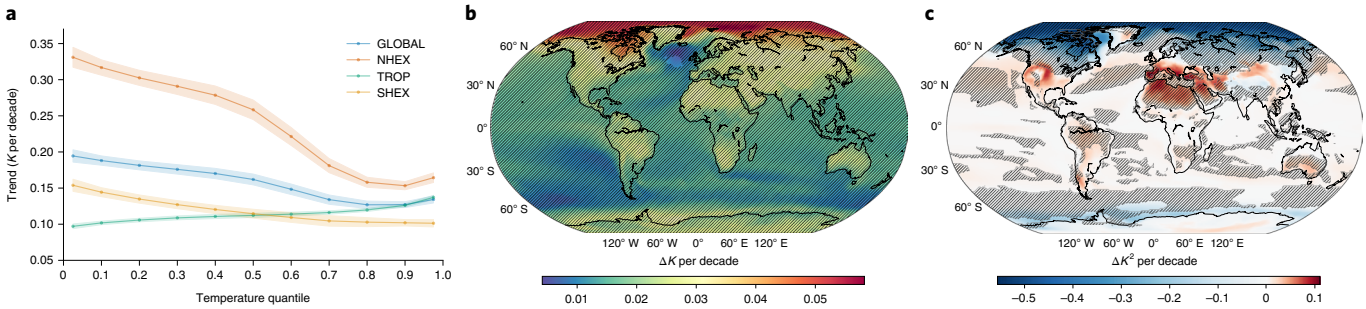

Fig. 2 | Mean trends in the statistical distribution of daily air temperature between 1850 and 2100. a,**b**, Trends in the percentile values of air temperature (**a**, *K* per decade) and mean temperature at each geographic location (**b**, Δ*K* per decade) indicate asymmetrically warming temperature distributions in the Northern Hemisphere Extra-tropics (NHEX, 30° N to 90° N), the Tropics (TROP, 30° S to 30° N), the Southern Hemisphere Extra-tropics (SHEX, 90° S to 30° S), and the full globe (GLOBAL, 90° S to 90° N). Shaded bounds denote the 90% confidence interval based on eight CMIP6 models. **c**, Trends in the variance of daily air temperature (ΔK^2 per decade) exhibit similarly complex regional patterns. The concurrent decrease in variability at high latitudes and increase at other latitudes suggests that temperature variation is becoming more spatially homogeneous in a warming world. Hashed contours indicate statistically significant inter-model agreement on the sign of the trend at the $\alpha = 0.05$ significance level.

temporal autocorrelation (decreasing spectral exponent) at a majority of sea locations (60%) and land locations (80%), excluding Antarctica where autocorrelation is decreasing. Autocorrelation is increasing most rapidly in equatorial land areas including the Amazon and the Southeast Asian islands, with high inter-model agreement on the sign of the trend. Notable exceptions to the increasing trend in autocorrelation include Greenland, Western Africa, Western Europe and parts of Central Asia. Generally, agreement between models is higher at mid latitudes than in the polar zones or the tropics, where climate model bias and spread have historically persisted[30]. Regional analysis indicates statistically significant increasing trends in temporal autocorrelation in NHEX (-1.12×10^{-3} per decade, $P = 0.010$), TROP (-1.14×10^{-3} per decade, $P = 0.001$) and globally (-0.54×10^{-3} per decade[1], $P = 0.005$), and a statistically significant decreasing trend in temporal autocorrelation in SHEX (0.53×10^{-3} per decade, $P = 0.009$; Supplementary Table 1). The direction and significance of these trends are consistent across land and sea environments, although the spectral exponent is more negative for sea than land, probably due to the buffering effects of the ocean (Fig. 3b–e). In NHEX and TROP, autocorrelation is increasing at a greater rate in land locations than in sea locations, while in SHEX it is decreasing at similar rates between land and sea (Supplementary Table 2). A greater degree of temporal autocorrelation is associated with more gradual changes of state and, even without any changes in variance, results in longer durations spent under extreme conditions. A greater clustering of similar temperatures has been suggested to increase exposure to heat waves and cold snaps while decreasing the incidence of protective temporal refugia[20].

Regional differences in warming patterns

In the northern latitudes, variance and autocorrelation exhibit opposite temporal trends. The decreasing variance may be attributed to a decrease in high-frequency variability and more rapid warming of the lower than the upper quantiles of the temperature distribution. Studies of reanalysis data and observations have also implicated decreasing cold-season sub-seasonal variability and rapidly warming cold days in decreasing temperature variability in mid to high northern latitudes[20,24,29]. Meanwhile, temporal autocorrelation in NHEX is increasing—a finding that has also been detected in the previous generation of climate models[20], weather station observations[31] and monthly reanalysis data[19]. As a result, variation at 2 d to 10 yr periodicities is decreasing while temperature fluctuations are becoming more persistent, suggesting the increased probability of a series of homogeneous conditions. In contrast to the mid to high northern latitudes, variance and temporal autocorrelation show similar trends at most latitudes, that is, both variance and autocorrelation are increasing.

Implications for global ectotherm populations

To better understand the independent and joint effects of these projected trends in the mean, variance and autocorrelation of temperature on ecological systems, we used empirical thermal performance information from invertebrate ectotherms compiled by Deutsch et al.[5]. We extracted temperature time series from the eight CMIP6 climate models at geographical point locations corresponding to the source sites of the 38 species (Fig. 4a). A dynamical population simulation using species-specific temperature-dependent growth rates yielded time series of population abundance for the historical period (1950–2000) and the latter half of the twenty-first century (2050–2100). We used a dynamical logistic growth model whose carrying capacity $K = r_t/\alpha$ is determined by the temperature-dependent growth rate r_t and the self-regulation parameter α. Importantly, the model captures the effects of temperatures above the critical thermal maximum and extinction propensity under autocorrelated variation by allowing growth rates to become negative (see Methods for details). Using the eight climate simulations as replicates, we compared the historical and future periods to detect statistically significant temperature-driven changes in population abundance, stability (mean/standard deviation of abundance) and extinction probability (proportion of simulations where a species did not have a strictly positive final abundance).

Under the high emissions scenario (SSP5-8.5), population abundance increased for the plurality of species (18 of 38) because the mean temperature grew closer to their thermal optimum and thus boosted equilibrium abundance, but it decreased for 10 species (Supplementary Table 3). Population abundance increased significantly for all TROP species (5 of 5) and for the majority (5 of 8) of SHEX species. In NHEX, outcomes were mixed, with approximately equal proportions of species experiencing an increase in abundance, a decrease in abundance, and no significant change. NHEX population abundance followed latitudinal patterns, generally decreasing between 30° N and 45° N, and increasing above of 45° N. Under the high emissions scenario, population stability increased for the plurality of species (16 of 38) and decreased for 10 species (Fig. 4b). Population stability increased or underwent no significant change for TROP species, while in the mid latitudes (NHEX and SHEX), changes in stability were mixed. Additional analyses showed that the trends in stability were mainly due to the emergence of two distinct dynamical regimes under climate change, with species either moving to a low-mean/low-variance mode or a high-mean/high-variance mode, particularly in the extra-tropics

https://doi.org/10.1038/s41558-022-01490-7

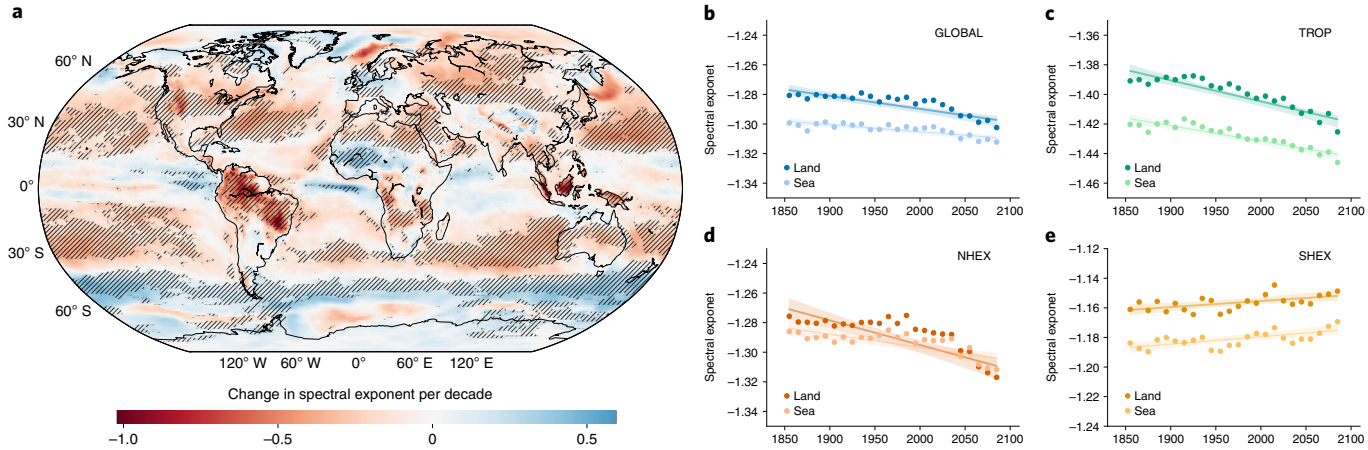

Fig. 3 | Increasing temporal autocorrelation in daily air temperature between 1850 and 2100. a, Spatiotemporal trends in temporal autocorrelation suggest changes in the chronological sequence of temperature conditions, with increasing temporal autocorrelation (decreasing spectral exponent) at 80.04% of global land locations, excluding Antarctica. Hashed contours indicate statistically significant inter-model agreement on the sign of the trend at the $\alpha = 0.05$ significance level. **b**–**e**, Regional analysis indicates statistically significant increasing trends in temporal autocorrelation in NHEX and TROP, and a statistically significant decreasing trend in temporal autocorrelation in SHEX. While sea environments generally exhibit a greater degree of temporal autocorrelation than land, in NHEX autocorrelation is increasing at a greater rate on land locations as to overturn this relationship by the end of the twenty-first century.

(Extended Data Figs. 2 and 3). These results were robust to orders of magnitude changes in the growth rate r_t and self-regulation parameter α (Extended Data Figs. 4 and 5).

Many SHEX and NHEX species suffered performance losses (negative growth rates) during summers in their respective hemispheres, as they are generally less tolerant of hot temperatures than tropical species. For some temperate species, longer growing seasons and warmer winter temperatures offset the negative effect of the warmest part of the year, while others suffered an overall performance loss[32]. This is consistent with the suggestion that increases in summer heat stress would reduce overall fitness and increase fitness variation for many mid-latitude species. Our results suggest that temperate species may be at greater risk than tropical species as a result of warm days, even when annual mean temperature remains below the thermal optimum. The results contrast with those of previous studies, which suggested on the basis of hourly temperature records and monthly temperature anomalies that warming in the tropics would be more deleterious than warming in the mid latitudes[5,33]. This discrepancy may be due to the fact that growth rates were allowed to become negative when temperatures exceeded the critical thermal maximum in our simulations but assumed to converge to zero (that is, were not allowed to be negative) in previous studies[4]. Our results are more consistent with studies that predict a greater risk of performance loss for temperate species when accounting for negative performance values in response to climate-mediated changes in the mean and the variance of temperature[15].

To tease apart the dynamical effects of climate change on population stability from its effects on mean performance as inferred by measuring average growth rate using each species' TPC, we replicated previous efforts by comparing changes in the average growth rate under historical and future climatic conditions with vs without negative growth rates (Extended Data Fig. 6). Our results show that although allowing negative growth rates predictably leads to greater reductions in performance overall, the regional patterns in performance are similar to the trends in population stability observed in the dynamical simulations, with tropical species generally enjoying performance gains and temperate species—particularly in NHEX—suffering performance losses (Extended Data Fig. 6).

Our simulations indicated mean warming as the dominant driver of ecological impacts. Changes in temporal autocorrelation alone (mean temperature and variance held at historical levels) had no significant effects on population abundance and a significant destabilizing effect on just 3 NHEX species. Changes in temporal autocorrelation and variance (mean temperature held at historical levels) led to a decrease in population abundance in 2 NHEX species and a decrease in population stability in 5 NHEX species. These results suggest that NHEX species are more vulnerable to negative effects of changes in temperature variability than TROP or SHEX species. Finally, changes in mean and temporal autocorrelation (variance held at historical levels) led to increased population abundance in 19 global species and increased stability in 19 global species, versus 18 and 16 under the high emissions scenario-projected changes in all three aspects of temperature. Thus, projected changes in temperature variability have a weak moderating effect on the positive effects of mean warming on population abundance and stability.

To determine how these complex changes in population abundance and stability translate to persistence, we quantified extinction risk as the proportion of the 8 CMIP6 models for which population abundance declined below an arbitrarily small threshold of 1×10^{-9} at any point during the 50 yr simulation (Fig. 4c). In our simulations under the high emissions scenario, extinction risk increased significantly under future climate conditions relative to historical baselines for 25 species, increased (but not significantly) for 13 species, and decreased for 0 species. We found statistically significant increases in extinction risk globally (Mann–Whitney $U = 376$, $n_1 = n_2 = 38$, $P = 6 \times 10^{-5}$) and in NHEX (Mann–Whitney $U = 150.5$, $n_1 = n_2 = 25$, $P = 5 \times 10^{-4}$). These findings suggest that temperature changes promote extinction risk, despite having a largely positive or neutral effect on population abundance and idiosyncratic impacts on stability. Hence, although variability among climate models produces a wide range of changes in stability across species and geographical locations, uncertainty at the climate level yields consistent biological impacts in the form of systematically higher extinction risks (Extended Data Fig. 7).

Conclusion

By forcing simple strategic and dynamical models of population growth with fine temporal scale temperature projections from the latest generation of Earth System Models, we demonstrated increased extinction risk under climate change across globally distributed ectotherm populations. Unfortunately, using more complex tactical dynamical models would require extensive species-, age- and life-stage-specific information about the effects of temperature fluctuations on population

https://doi.org/10.1038/s41558-022-01490-7

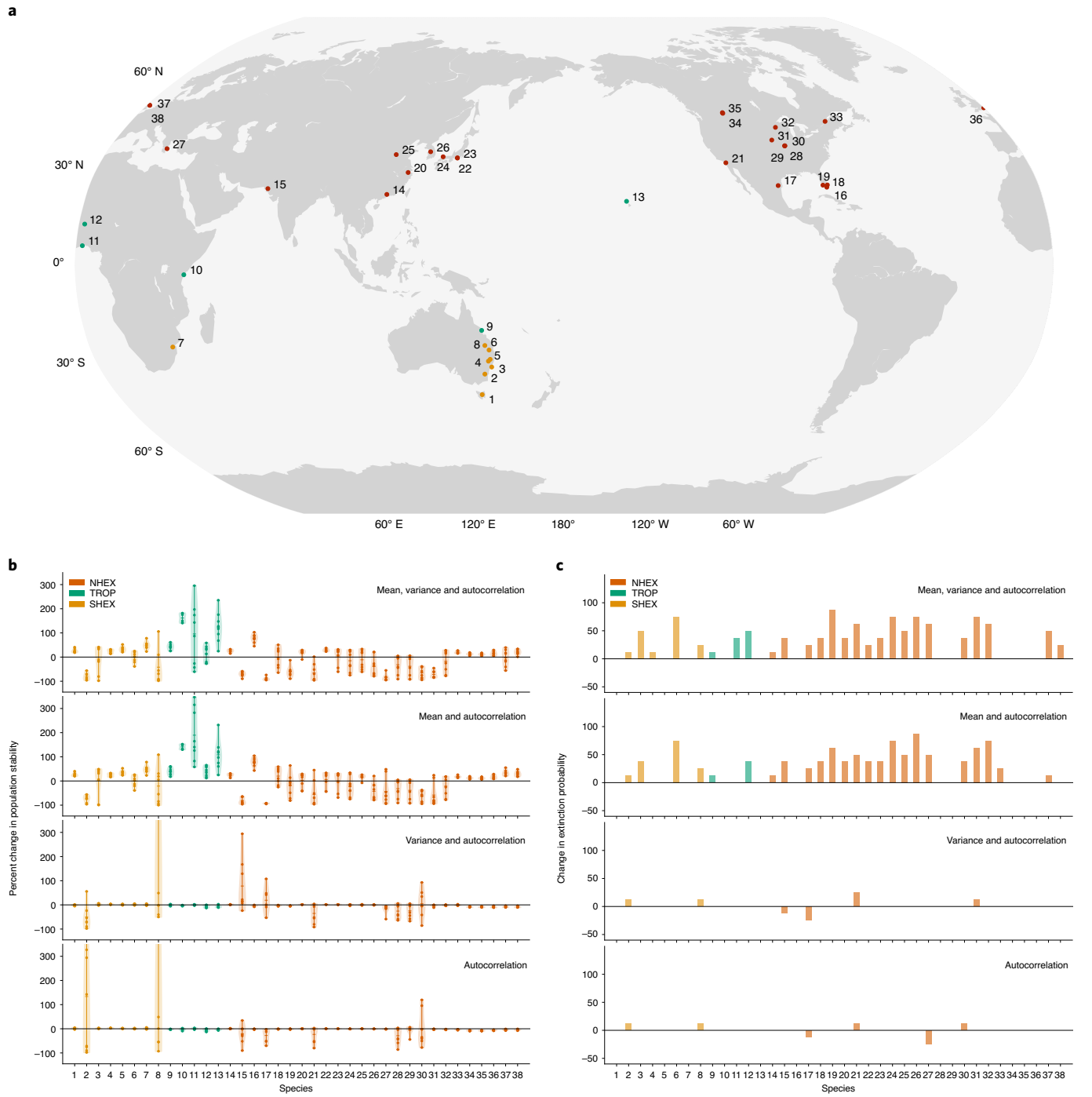

Fig. 4 | Temperature has idiosyncratic effects on stability but increases extinction risk globally. a, Source locations of the terrestrial ectothermic invertebrate species, numbered 1 (southernmost latitude) to 38 (northernmost latitude). Species are colour-coded according to latitudinal region (orange, SHEX; green, TROP; red, NHEX). **b**, Percent changes in population stability (mean ÷ s.d.) between a historical reference period (1950–2000) and a future period (2050–2100) under multiple aspects of temperature change indicate greater risk to temperate than to tropical species. Under a high emissions scenario, stability shows a statistically significant increase for the plurality (16 of 38) of species and a statistically significant decrease for 10 species. Points in the violin plots represent the 8 climate model outputs. **c**, Extinction probability shows a quasi-universal increase globally between the historical period (1950–2000) and a future period (2050–2100) under high emissions scenario changes in temperature.

growth rates that is simply not available at the relevant scales. Tactical models would also need to consider thermoregulation[34], the effects of microclimates[35], acclimatization or adaptation[36], partitioning of activity periods[37] and synecological processes such as predator-prey interactions that could affect ectotherm population dynamics. Additionally, due to their 1° spatial resolution, the climate projections used in this study are much coarser than the microclimates experienced by individual organisms and may thus lead to underestimates of organismal performance due to the presence of thermal refugia in the real world[23,34]. Hence, our results should be viewed as a qualitative baseline prediction of how the spatiotemporal distribution of extinction risk is likely to shift due to climate change rather than a quantitative forecast of when each species is likely to be extirpated from each geographical location.

Despite the limitations of TPCs in accounting for temporal carryover and dynamical effects, the lack of obvious alternatives calls for strategies to make these approaches more robust to real-world conditions[38], such as by integrating more realistic, fine-scaled temperature variation into our predictive models than previous studies. Although bioclimate envelope approaches have been criticized for not accounting for important ecological factors, such as species interactions and dispersal, when attempting to predict the ecological effects of climate change[39–42], we have shown that even under ideal conditions when the influence of such factors can be assumed to be negligible, statistical frameworks that ignore the dynamical consequences of temperature variation are likely to yield inaccurate forecasts of the impact of climate change on organisms. Our results show that accounting for shifts in the entire statistical distribution of temperature over time via dynamical models can better capture the cumulative effects of climate-mediated changes in thermal stress on extinction risk.

By bringing together climate data and a minimal dynamical model from ecology, we demonstrated a strong and systematic amplification of extinction risk in ectotherms due to projected changes in fine-grained temperature variability. Furthermore, our finding of greater risk to sub-tropical than tropical species highlights the importance of accounting for the dynamical effects of projected changes in the mean as well as the variance of temperature over the course of the twenty-first century to accurately predict the response of ecological systems around the globe.

Online content

Any methods, additional references, Nature Research reporting summaries, source data, extended data, supplementary information, acknowledgements, peer review information; details of author contributions and competing interests; and statements of data and code availability are available at https://doi.org/10.1038/s41558-022-01490-7.

References

1. *The Global Risks Report 2021 Insight Report* 16th edn (World Economic Forum, 2021).
2. Bellard, C., Bertelsmeier, C., Leadley, P., Thuiller, W. & Courchamp, F. Impacts of climate change on the future of biodiversity. *Ecol. Lett.* **15**, 365–377 (2012).
3. Parmesan, C. Ecological and evolutionary responses to recent climate change. *Annu. Rev. Ecol. Evol. Syst.* **37**, 637–669 (2006).
4. Pearson, R. G. & Dawson, T. P. Predicting the impacts of climate change on the distribution of species: are bioclimate envelope models useful? *Glob. Ecol. Biogeogr.* **12**, 361–371 (2003).
5. Deutsch, C. A. et al. Impacts of climate warming on terrestrial ectotherms across latitude. *Proc. Natl Acad. Sci. USA* **105**, 6668–6672 (2008).
6. Cheung, W. W. L. et al. Projecting global marine biodiversity impacts under climate change scenarios. *Fish Fish.* **10**, 235–251 (2009).
7. Thuiller, W. et al. Consequences of climate change on the tree of life in Europe. *Nature* **470**, 531–534 (2011).
8. Angilletta, M. J. *Thermal Adaptation: A Theoretical and Empirical Synthesis*. *Thermal Adaptation* (Oxford Univ. Press, 2009).
9. Ruel, J. J. & Ayres, M. P. Jensen's inequality predicts effects of environmental variation. *Trends Ecol. Evol.* **14**, 361–366 (1999).
10. Lawson, C. R., Vindenes, Y., Bailey, L. & Pol, Mvande Environmental variation and population responses to global change. *Ecol. Lett.* **18**, 724–736 (2015).
11. Denny, M. The fallacy of the average: on the ubiquity, utility and continuing novelty of Jensen's inequality. *J. Exp. Biol.* **220**, 139–146 (2017).
12. Denny, M. Performance in a variable world: using Jensen's inequality to scale up from individuals to populations. *Conserv. Physiol.* **7**, coz053 (2019).
13. García-Carreras, B. & Reuman, D. C. Are changes in the mean or variability of climate signals more important for long-term stochastic growth rate? *PLoS ONE* **8**, e63974 (2013).
14. Benedetti-Cecchi, L., Bertocci, I., Vaselli, S. & Maggi, E. Temporal variance reverses the impact of high mean intensity of stress in climate change experiments. *Ecology* **87**, 2489–2499 (2006).
15. Vasseur, D. A. et al. Increased temperature variation poses a greater risk to species than climate warming. *Proc. R. Soc. B* **281**, 20132612 (2014).
16. Schwager, M., Johst, K. & Jeltsch, F. Does red noise increase or decrease extinction risk? Single extreme events versus series of unfavorable conditions. *Am. Nat.* **167**, 879–888 (2006).
17. Kingsolver, J. G., Diamond, S. E. & Buckley, L. B. Heat stress and the fitness consequences of climate change for terrestrial ectotherms. *Funct. Ecol.* **27**, 1415–1423 (2013).
18. Meehl, G. A. More Intense, more frequent, and longer lasting heat waves in the 21st century. *Science* **305**, 994–997 (2004).
19. Lenton, T. M., Dakos, V., Bathiany, S. & Scheffer, M. Observed trends in the magnitude and persistence of monthly temperature variability. *Sci. Rep.* **7**, 5940 (2017).
20. Di Cecco, G. J. & Gouhier, T. C. Increased spatial and temporal autocorrelation of temperature under climate change. *Sci. Rep.* **8**, 14850 (2018).
21. Li, J. & Thompson, D. W. J. Widespread changes in surface temperature persistence under climate change. *Nature* **599**, 425–430 (2021).
22. Lembrechts, J. J. et al. Comparing temperature data sources for use in species distribution models: from in-situ logging to remote sensing. *Glob. Ecol. Biogeogr.* **28**, 1578–1596 (2019).
23. Potter, K. A., Arthur Woods, H. & Pincebourde, S. Microclimatic challenges in global change biology. *Glob. Change Biol.* **19**, 2932–2939 (2013).
24. O'Neill, B. C. et al. The Scenario Model Intercomparison Project (ScenarioMIP) for CMIP6. *Geosci. Model Dev.* **9**, 3461–3482 (2016).
25. Hansen, J., Sato, M. & Ruedy, R. Perception of climate change. *Proc. Natl Acad. Sci. USA* **109**, E2415–E2423 (2012).
26. Bathiany, S., Dakos, V., Scheffer, M. & Lenton, T. M. Climate models predict increasing temperature variability in poor countries. *Sci. Adv.* **4**, eaar5809 (2018).
27. Screen, J. A. Arctic amplification decreases temperature variance in northern mid- to high-latitudes. *Nat. Clim. Change* **4**, 577–582 (2014).
28. Stouffer, R. J. & Wetherald, R. T. Changes of variability in response to increasing greenhouse gases. Part I: temperature. *J. Clim.* **20**, 5455–5467 (2007).
29. Gouhier, T. C. & Pillai, P. Commentary: nonlinear averaging of thermal experience predicts population growth rates in a thermally variable environment. *Front. Ecol. Evol.* **7**, 236 (2019).
30. Tian, B. & Dong, X. The double-ITCZ bias in CMIP3, CMIP5, and CMIP6 models based on annual mean precipitation. *Geophys. Res. Lett.* **47**, e2020GL087232 (2020).
31. Dillon, M. E. et al. Life in the frequency domain: the biological impacts of changes in climate variability at multiple time scales. *Integr. Comp. Biol.* **56**, 14–30 (2016).
32. Adamo, S. A., Baker, J. L., Lovett, M. M. E. & Wilson, G. Climate change and temperate zone insects: the tyranny of thermodynamics meets the world of limited resources. *Environ. Entomol.* **41**, 1644–1652 (2012).
33. Dillon, M. E., Wang, G. & Huey, R. B. Global metabolic impacts of recent climate warming. *Nature* **467**, 704–706 (2010).
34. Sunday, J. M. et al. Thermal-safety margins and the necessity of thermoregulatory behavior across latitude and elevation. *Proc. Natl Acad. Sci. USA* **111**, 5610–5615 (2014).

35. Pincebourde, S. & Casas, J. Narrow safety margin in the phyllosphere during thermal extremes. *Proc. Natl Acad. Sci. USA* **116**, 5588–5596 (2019).
36. Somero, G. N. The physiology of climate change: how potentials for acclimatization and genetic adaptation will determine 'winners' and 'losers'. *J. Exp. Biol.* **213**, 912–920 (2010).
37. Johansson, F., Orizaola, G. & Nilsson-Örtman, V. Temperate insects with narrow seasonal activity periods can be as vulnerable to climate change as tropical insect species. *Sci. Rep.* **10**, 8822 (2020).
38. Sinclair, B. J. et al. Can we predict ectotherm responses to climate change using thermal performance curves and body temperatures? *Ecol. Lett.* **19**, 1372–1385 (2016).
39. Davis, A. J., Jenkinson, L. S., Lawton, J. H., Shorrocks, B. & Wood, S. Making mistakes when predicting shifts in species range in response to global warming. *Nature* **391**, 783–786 (1998).
40. Suttle, K. B., Thomsen, M. A. & Power, M. E. Species interactions reverse grassland responses to changing climate. *Science* **315**, 640–642 (2007).
41. Gouhier, T. C., Guichard, F. & Menge, B. A. Ecological processes can synchronize marine population dynamics over continental scales. *Proc. Natl Acad. Sci. USA* **107**, 8281–8286 (2010).
42. Harley, C. D. G. Climate change, keystone predation, and biodiversity loss. *Science* **334**, 1124–1127 (2011).

Methods

CMIP6 simulations

We obtained CMIP6 climate simulations for the historical forcing period (1850–2014) and future emissions scenario SSP5-8.5 (2015–2100) via the CMIP6 data portal (https://esgf-node.llnl.gov/search/cmip6/). Eight models from CMIP6 (AWI-CM-1-1-MR, BCC-CSM2-MR, CESM2, EC-Earth3, INM-CM5-0, MPI-ESM1-2-HR, MRI-ESM2-0 and NorESM2-MM) were selected on the basis of availability of daily air temperature at surface ('tas') at a 100 km nominal resolution at the time of download. While 'tas' at sub-daily frequencies is available for some models, daily data was selected to maximize the ensemble size. We resampled all datasets to a common 1° by 1° grid spanning −90° to 90° latitude and 0° to 360° longitude, and to a standard calendar without leap years. Spatial regions were defined on the basis of latitude as Northern Hemisphere Extra-tropics (90° S to 30° S), Tropics (30° S to 30° N) and Southern Hemisphere Extra-tropics (30° N to 90° N).

Statistical analyses of climate data

Quantile regression. Trends in the percentile values of global and regional temperature distributions were computed via quantile regression. Quantile regression can comprehensively model heterogeneous conditional distributions, where the relationship between the quantiles of the dependent variable and the independent variable is different from the relationship between the means of the dependent variable and the independent variable. We applied quantile regression to analyse trends with respect to time at various percentile values ($P_{2.5}$, P_{10}, P_{20}, P_{30}, P_{40}, P_{50}, P_{60}, P_{70}, P_{80}, P_{90}, $P_{97.5}$). Analyses were performed using the R package quantreg, with significance level $\alpha = 0.1$ and the default Barrodale and Roberts method to return confidence intervals for the estimated parameters. To obtain the ensemble mean trends, we calculated the mean slope, upper bound and lower bound across the eight climate models at each geographical location, then computed spatial averages for the full globe and three latitudinal regions.

Variance. Trends in the magnitude of temporal variation of air temperature were examined at each geographical location using a moving window approach. First, temperature was detrended by fitting a piecewise linear regression against time with Python package pwlf at each geographical location and extracting the residuals. Then, the temperature time series were divided into 10 yr windows starting in years 1855 through 2085 so as not to combine historical and future simulations (pre- and post-01-01-2015), and the variance of daily air temperature was calculated for each window. Windows were selected with no overlap to avoid statistical issues due to non-independence of estimates taken from partially overlapping time windows[20].

Scale-specific variability. Scale-specific variability was quantified using time-frequency decomposition. Specifically, at each geographical location, wavelet analysis was conducted on multi-model mean temperature using the R package biwavelet[43]. Wavelet analysis resolves both the time and frequency domains of a signal (here a time series) via the wavelet transform. This is achieved via the convolution of a mother wavelet function and a time series across a set of windows τ and scales s. We chose to use the Morlet wavelet, which represents a sine wave modulated by a Gaussian function:[44]

$$\psi_0(t) = \pi^{-1/4} e^{i\omega_0^t} e^{-t^2/2}$$

where i is the imaginary unit, t represents non-dimensional time, and $\omega_0 = 6$ is the non-dimensional frequency[3]. The continuous wavelet transform of a discrete time series $x(t)$ with equal spacing δt and length T is defined as the convolution of $x(t)$ with a normalized Morlet wavelet:[44,45]

$$W_x(s,\tau) = \sqrt{\frac{\delta t}{s}\sum_{t=0}^{T-1} x(t)\,\psi_0 * \left(\frac{(t-\tau)\,\delta t}{s}\right)}$$

where * indicates the complex conjugate. By varying the wavelet scale s (that is, dilating and contracting the wavelet) and translating along localized time position τ, one can calculate the wavelet coefficients $W_x(s,\tau)$ across the different scales s and positions τ. These wavelet coefficients can be used to compute the bias-corrected local wavelet power, which describes how the contribution of each frequency or period in the time series varies over time:[44,46,47]

$W_x^2(s,\tau) = 2^s |W_x(s,\tau)|^2$ where 2^s is the bias correction factor[46]. The scale s of the Morlet wavelet is related to the Fourier frequency f:[47,48]

$\frac{1}{f} = \frac{4\pi s}{\omega_0 + \sqrt{2+\omega_0^2}}$.

When $\omega_0 = 6$, the scale s is approximately equal to the reciprocal of the Fourier frequency f, so period $p \approx s$. The local wavelet power spectrum can then be visualized via heat maps and contour plots[45,47]. From the resulting local wavelet power spectrum heat map with time on the x axis, period (scale) on the y axis and power on the z axis, scale-averaged wavelet power was computed at annual (between 3 d and 2 yr) and multi-annual (between 2 yr and 30 yr) periodicities. This was achieved by taking the weighted sum of the local wavelet power across all scales for each time location τ:[44,47]

$$W_x^2(\tau) = \frac{\delta j \delta t}{C_\delta}\sum_{j=0}^{J}\frac{|W_x(s_j,\tau)|^2}{s_j}$$

where $C_\delta = 0.776$ for the Morlet wavelet, δJ represents the spacing between successive scales and δt represents the spacing between successive time locations[44]. Scale-averaged power was then regressed against time using Generalized Least Squares (GLS) regression for the period 1850–2100 at each geographic location. To determine the robustness of results to the choice of period for scale averaging, we also performed analysis of trends separately at interannual (between 2 yr and 7 yr) and multi-annual (between 7 yr and 30 yr) scales and found qualitatively similar results.

Temporal autocorrelation. The temporal autocorrelation of air temperature was quantified by calculating the spectral exponent at each geographical location[20]. As described above, temperature was detrended by fitting a piecewise linear regression at each geographical location and extracting the residuals. The detrended temperature was divided into 10 yr windows starting in years 1855 through 2085. Fourier transforms of each time series were computed via fast Fourier transform using the Python package NumPy. Periodograms were prepared with frequency on the x axis and power spectral density on the y axis. The spectral exponent, β, was calculated as the slope of the regression line relating log-transformed power to log-transformed frequency. β expresses the relative contributions of frequencies to the power spectrum. In the case of equal contribution from all frequencies, $\beta = 0$. Greater contribution from low frequencies than from high frequencies results in a more negative value of β and indicates greater temporal autocorrelation in the time domain.

Analysis of decadal trends. For each climate model, GLS regression was used to detect statistically significant trends ($P < 0.05$) in variance and temporal autocorrelation with respect to time in the presence of potentially autocorrelated residuals. To measure inter-model agreement, we calculated the multi-model mean trend as the mean of trends calculated for each of the 8 models at each geographic location, then assessed the proportion of models that agreed with the sign of the multi-model mean trend. Inter-model agreement was considered as statistically significant at the $\alpha = 0.1$ level on the basis of a binomial test. ANCOVA was used to quantify the relationship between temporal

autocorrelation and time while accounting for potential differences between land and sea environments. Statistically significant main effects and interactions were reported for $P < 0.05$.

Modelling temperature impacts on ecology

Thermal tolerance data. We obtained experimentally derived thermal tolerance parameters for a set of terrestrial ectotherms ($n = 38$) published by Deutsch et al.[5] and used them to predict physiological response to CMIP6-simulated temperature. Deutsch et al.[5] gathered data from 31 thermal performance studies published between 1974 and 2003 based on a collection of insects from 35 different locations. For each species, experimental intrinsic growth rates at multiple temperatures were used to fit a TPC, yielding least-squares estimates of key parameters such as critical thermal maximum (CT_{max}), optimum temperature (T_{opt}), and sigma (σ). We used a numerical scheme to reconstruct the curves whereby the rise in performance up to T_{opt} was modelled as Gaussian and the decline beyond T_{opt} was quadratic[5,49]:

$$P(T) = \begin{cases} \exp\left[-\left(\frac{T-T_{opt}}{2\sigma}\right)^2\right] & \text{for } T \le T_{opt} \\ 1-\left(\frac{T-T_{opt}}{T_{opt}-CT_{max}}\right)^2 & \text{for } T > T_{opt} \end{cases}. \quad (1)$$

This allowed negative growth rates to arise at high temperatures, but growth rates were bound at zero at low temperatures. Negative performance values indicate that mortality surpasses reproduction rates. Because $P(T)$ is capped at 1 under this numerical scheme, $P(T)$ represents the relative fitness of each species based on its normalized maximum growth rate. However, scaling this relative or normalized maximum growth rate by two orders of magnitude (that is, by a factor of 0.1 or 10.0) had limited quantitative and no qualitative impact on our results (Extended Data Fig. 4). Overall, increasing the growth rate scaling factor had no impact on population stability but promoted extinction risk.

Isolation of temperature aspects. To isolate projected changes in mean temperature and variability, we transformed the future (2050–2100) time series using z-score normalization. Using this approach, we modified projected time series to match the historical (1950–2000) mean and/or standard deviation. Working in 10 yr moving windows between 2050 and 2100, each series x_i with mean m_1 and standard deviation s_1 was transformed to series y_i with mean m_2 and standard deviation s_2:

$$y_i = m_2 + (x_i - m_1)\frac{s_2}{s_1}. \quad (2)$$

According to the scenario, m_2 and s_2 were alternatively defined as (1) high emissions scenario mean and standard deviation ('Mean, variance and autocorrelation'), (2) high emissions scenario mean and historical standard deviation ('Mean and autocorrelation'), (3) historical mean and high emissions scenario standard deviation ('Variance and autocorrelation') and (4) historical mean and standard deviation ('Autocorrelation'). High emissions scenario statistics refer to the properties of future series x_i and confer no change to that aspect of the time series.

Population dynamical modelling. To model the effects of temperature change on the stability and extinction probability of global ectotherm populations, temperature dependence was integrated in the growth rate term of a population dynamical model[50]. While more complex synecological models can capture a range of community-level effects including competition and predation, we chose to model first order autecological dynamics to produce foundational insights about the role of temperature fluctuations on single-species population dynamics. Specifically, we used the $r-\alpha$ logistic growth model to simulate temperature-dependent growth and negative density-dependence:

$$\frac{dN}{dt} = N(r_t - \alpha N) \quad (3)$$

with population size N, time t, temperature-dependent growth rate r_t, and self-regulation in the form of intraspecific competition α. This $r-\alpha$ logistic model is easily interconvertible with the classical $r-K$ formulation ($r/\alpha = K$), but has the advantage of handling negative values of r without issues[51]. This approach is sensitive to the effects of temperatures at and above the critical thermal maximum, which can yield negative growth rates that are important for determining population dynamics as well as long-term fitness.

We extracted time series of daily temperature at the source locations for each species from the ensemble of eight climate simulations. Daily intrinsic growth rates were computed from temperature using equation (1), incorporated into the $r-\alpha$ logistic growth model depicted in equation (3), and the model was then numerically solved using the explicit Runge-Kutta method of order 5(4) implemented in the Python SciPy package to obtain daily population densities. Rather than delineating active periods, which may shift under climate change, we considered the full year to account for potential changes in fitness due to shifts in activity.

The sensitivity of the results to strong ($\alpha = 1$) and weak ($\alpha = 0.1$) self-regulation was examined and found to be extremely limited (Extended Data Fig. 5). We also assessed the sensitivity of our results to absolute rather than relative or normalized growth rates by scaling r_t by a factor of 0.1 or 10 in our simulations. Scaling r_t by two orders of magnitude in this manner had very little quantitative and no qualitive impact on our results. This suggests that the effects of temperature fluctuations on changes in the spatiotemporal distribution of population abundance, stability and extinction were not contingent upon the use of relative fitness (that is, normalized growth rate) versus absolute fitness (that is, growth rate scaled by a factor of 0.1 or 10). These sensitivity analyses also showed that our results are robust to temperature-mediated changes in the maximum instantaneous growth rate[52,53].

Analysis of population changes. To quantify temperature-driven changes in ecological stability and extinction probability, we compared population sizes and dynamics between a historical period (1950–2000) and a future period (2050–2100). Here we defined latitudinal regions according to traditional delineations in ecology: Northern Hemisphere Extra-tropics, 60° S to 23° S; Tropics, 23° S to 23° N; and Southern Hemisphere Extra-tropics, 23° N to 60° N.

Population abundance was computed as the mean population size (N) for a time period. Population stability was computed as the inverse of the coefficient of variation, or mean population divided by population standard deviation. Percent changes in population size and stability were computed for each of the climate models as $(\text{future} - \text{historical})/\text{historical} \times 100\%$ and plotted without outliers in Fig. 4. Statistically significant changes in population abundance and stability between the historical and future periods were identified via the Mann–Whitney U-test, with the eight models as replicates.

Extinction probability was quantified as the proportion of ensemble simulations for which the population declined to zero during a 50 yr simulation. Changes in extinction probability were calculated as the difference between future and historical extinction probabilities. Statistically significant changes in extinction probability were identified on a regional basis via the Mann–Whitney U-test.

Reporting summary

Further information on research design is available in the Nature Research Reporting Summary linked to this article.

Data availability

The CMIP6 simulation data used in this paper are available via the data portal https://esgf-node.llnl.gov/search/cmip6/. The ecology data are available for download at https://doi.org/10.1073/pnas.0709472105.

Code availability

The code can be accessed on GitHub at https://github.com/KateDuffy/climate-change-ecology[54].

References

43. Gouhier, T. C., Grinsted, A. & Simko, V. R package biwavelet: Conduct Univariate and Bivariate Wavelet Analyses (Version 0.20.17).
44. Torrence, C. & Compo, G. P. A practical guide to wavelet analysis. *Bull. Am. Meteorol. Soc.* **79**, 61–78 (1998).
45. Grinsted, A., Moore, J. C. & Jevrejeva, S. Application of the cross wavelet transform and wavelet coherence to geophysical time series. *Nonlinear Process. Geophys.* **11**, 561–566 (2004).
46. Liu, Y., Liang, X. S. & Weisberg, R. H. Rectification of the bias in the wavelet power spectrum. *J. Atmos. Ocean. Technol.* **24**, 2093–2102 (2007).
47. Cazelles, B. et al. Wavelet analysis of ecological time series. *Oecologia* **156**, 287–304 (2008).
48. Maraun, D. & Kurths, J. Cross wavelet analysis: significance testing and pitfalls. *Nonlinear Process. Geophys.* **11**, 505–514 (2004).
49. Huey, R. B. & Stevenson, R. D. Integrating thermal physiology and ecology of ectotherms: a discussion of approaches. *Am. Zool.* **19**, 357–366 (1979).
50. Mallet, J. The struggle for existence: how the notion of carrying capacity, K, obscures the links between demography, Darwinian evolution, and speciation. *Evol. Ecol. Res.* **14**, 627–665 (2012).
51. Vasseur, D. A. *Theoretical Ecology: Concepts and Applications* (eds. McCann, K. S. & Gellner, G.) 243–262 (Oxford Univ. Press, 2020).
52. Estay, S. A., Clavijo-Baquet, S., Lima, M. & Bozinovic, F. Beyond average: an experimental test of temperature variability on the population dynamics of *Tribolium confusum*. *Popul. Ecol.* **53**, 53–58 (2011).
53. Bozinovic, F. et al. The mean and variance of environmental temperature interact to determine physiological tolerance and fitness. *Physiol. Biochem. Zool.* **84**, 543–552 (2011).
54. Duffy, K. climate-change-ecology (GitHub, 2022); https://github.com/KateDuffy/climate-change-ecology

Acknowledgements

This work was primarily supported by the National Science Foundation (NSF) grant CCF-1442728 while K.D. was a PhD student at the SDS Lab in Northeastern University. Additional support was provided for K.D. and A.R.G. by NSF SES-1735505 and for T.C.G. by NSF OCE-2048894. We acknowledge the background support from a previous NSF Expeditions in Computing grant (award no. 1029711) and an ongoing DOD Strategic Environmental Research and Development Program funding (no. RC20-1183). K.D. and A.R.G. acknowledge support from the NASA Ames Research Center.

Author contributions

K.D., T.C.G. and A.R.G. conceived, designed and refined the project. K.D. performed the data analysis and modelling. K.D., T.C.G. and A.R.G. interpreted the results. K.D. wrote the manuscript with contributions from T.C.G. and A.R.G.

Competing interests

The authors declare no competing interests.

Additional information

Extended data is available for this paper at https://doi.org/10.1038/s41558-022-01490-7.

Supplementary information The online version contains supplementary material available at https://doi.org/10.1038/s41558-022-01490-7.

Correspondence and requests for materials should be addressed to Kate Duffy.

Peer review information *Nature Climate Change* thanks David Vasseur and the other, anonymous, reviewer(s) for their contribution to the peer review of this work.

https://doi.org/10.1038/s41558-022-01490-7

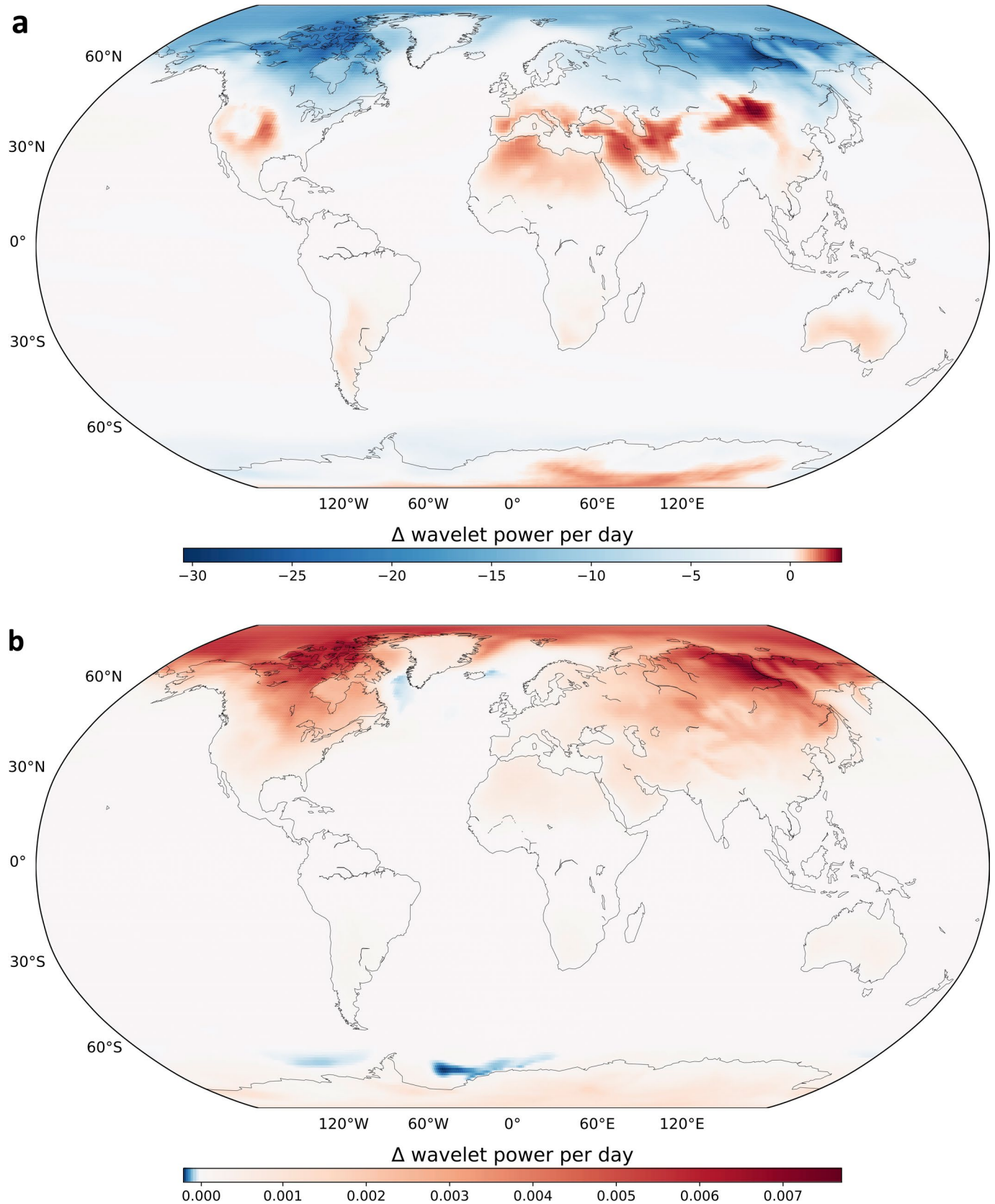

Extended Data Fig. 1 | Temperature variation at multiple timescales contributes to trends in overall variance. a-b Temporal trends in the power of variation at sub-annual to annual periodicities (3-days to 2-years) (**a**) and multi-annual periodicities (2-30 years) (**b**). Trends represent the slope obtained by regressing wavelet power at each geographical location against time. Countervailing trends are found in the Arctic, where the power of short term, high-frequency fluctuations is decreasing and the power of more persistent, low-frequency fluctuations is increasing.

https://doi.org/10.1038/s41558-022-01490-7

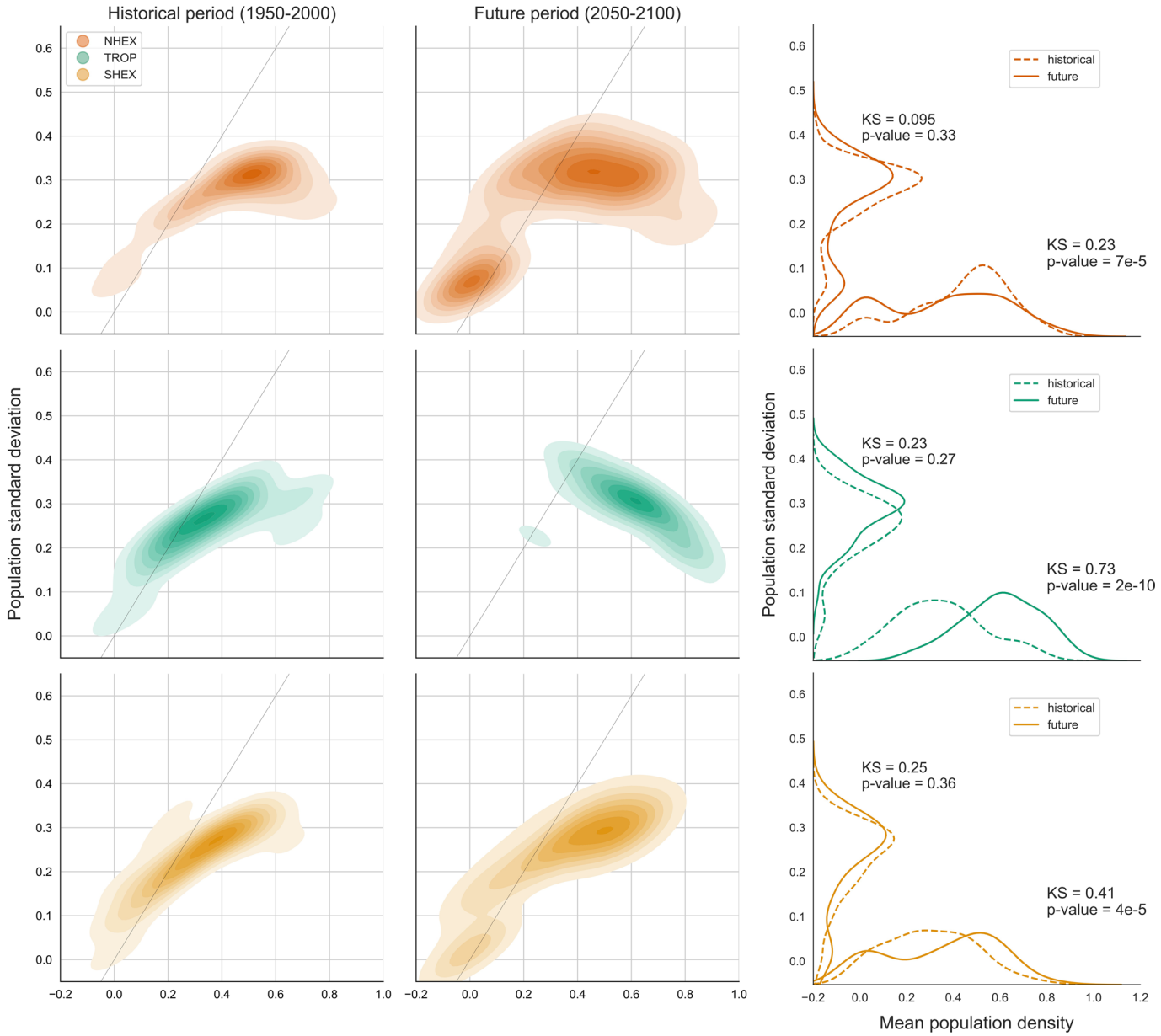

Extended Data Fig. 2 | Drivers of changes in stability (analysis includes both pre- and post-extinction period). Kernel density plots illustrate the relationships between population mean and population standard deviation in the historical period and the future climate change period. The grey 1:1 line divides the more stable regime (high-mean/low-variance; below line), and the less stable regime (low-mean/high-variance; above line). Bimodal distributions emerge in the extra-tropics, with some species at low abundance and standard deviation, and a larger cluster of species at high abundance and standard deviation. In the tropics, the emergence of two regimes is associated with significant increases in the distributions of both population abundance and standard deviation via the Kolmogorov-Smirnov test.

https://doi.org/10.1038/s41558-022-01490-7

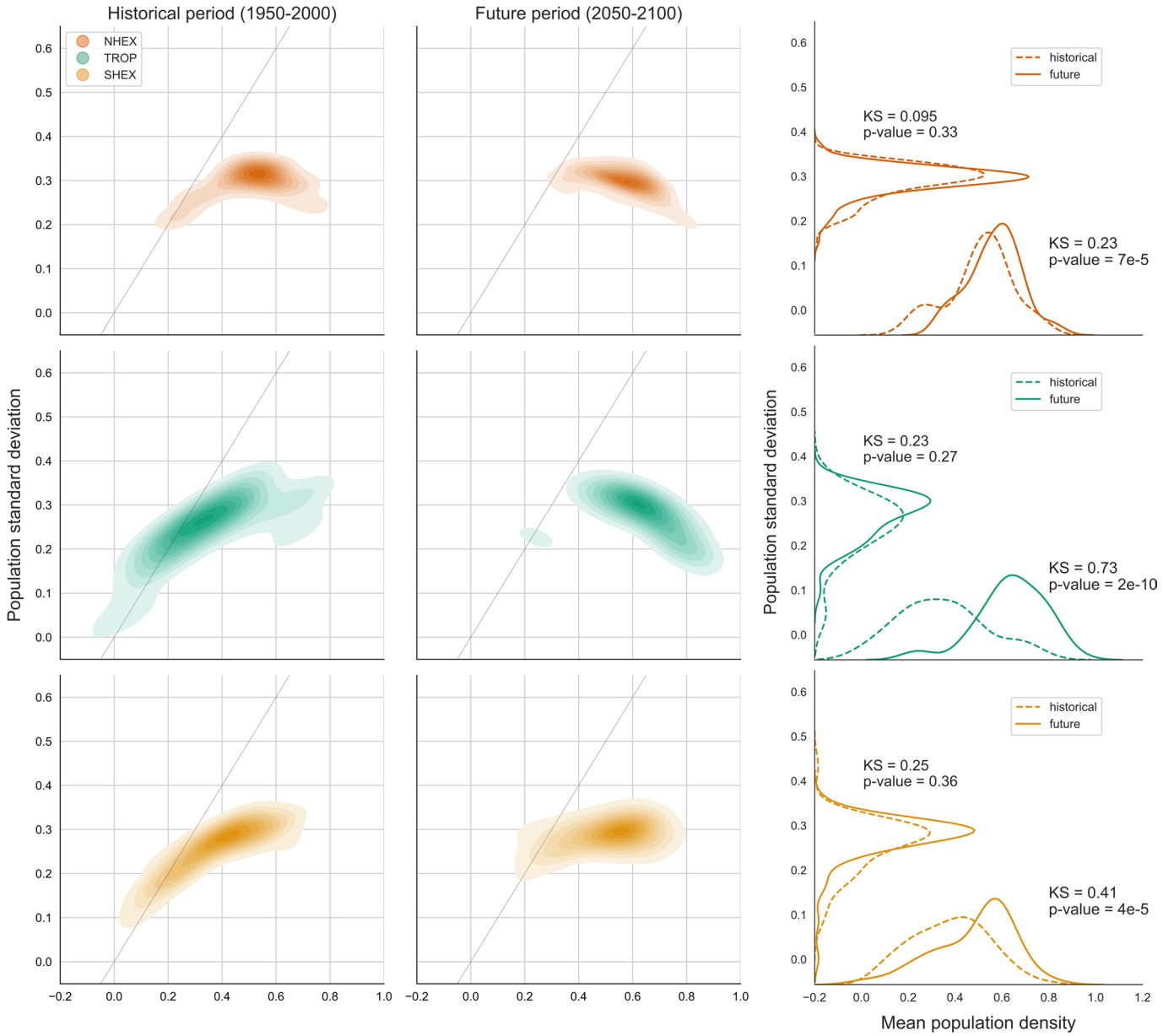

Extended Data Fig. 3 | Drivers of changes in stability (analysis only includes pre-extinction period). Although narrower distributions result for mean and standard deviation when only pre-extinction dynamics are analyzed, changes in the general patterns of stability regimes are consistent. Statistically significant changes in population abundance persist in all three regions; changes in population standard deviation become (remain) non-significant for NHEX and TROP (SHEX).

https://doi.org/10.1038/s41558-022-01490-7

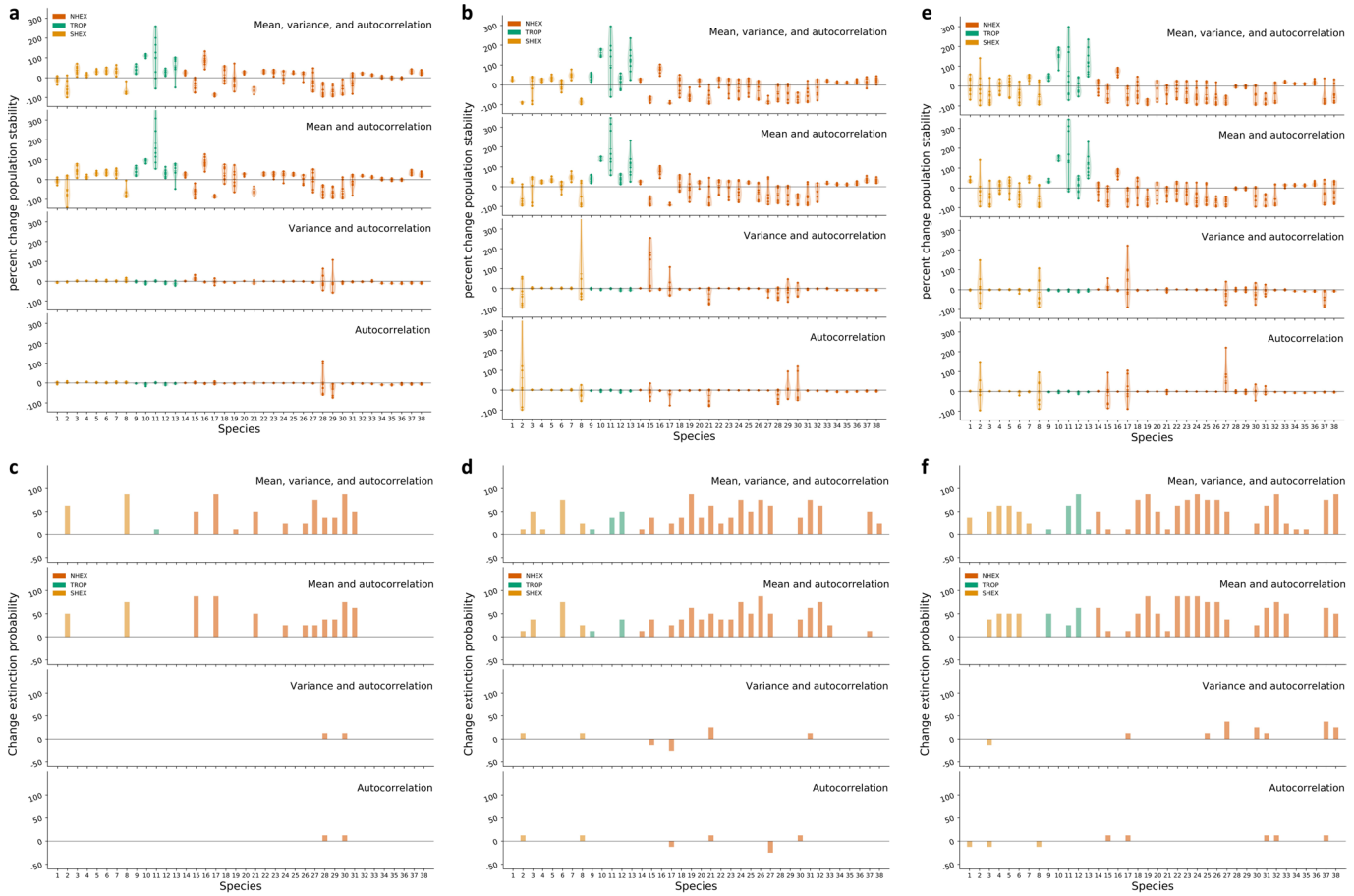

Extended Data Fig. 4 | Scaling of the intrinsic growth rate has moderate effects on temperature-driven impacts on population stability and extinction risk. Results exhibited limited sensitivity to the choice of smaller (scaling factor = 0.1; **a,b**) and larger (scaling factor = 10.0; **e,f**) intrinsic growth rates. Although larger growth rates were more strongly associated with deceased stability and increased extinction risk than smaller growth rates, the latitudinal patterns and effect sizes were consistent with the changes in population stability, **c**, and extinction probability, **d**, observed under normalized growth rates.

https://doi.org/10.1038/s41558-022-01490-7

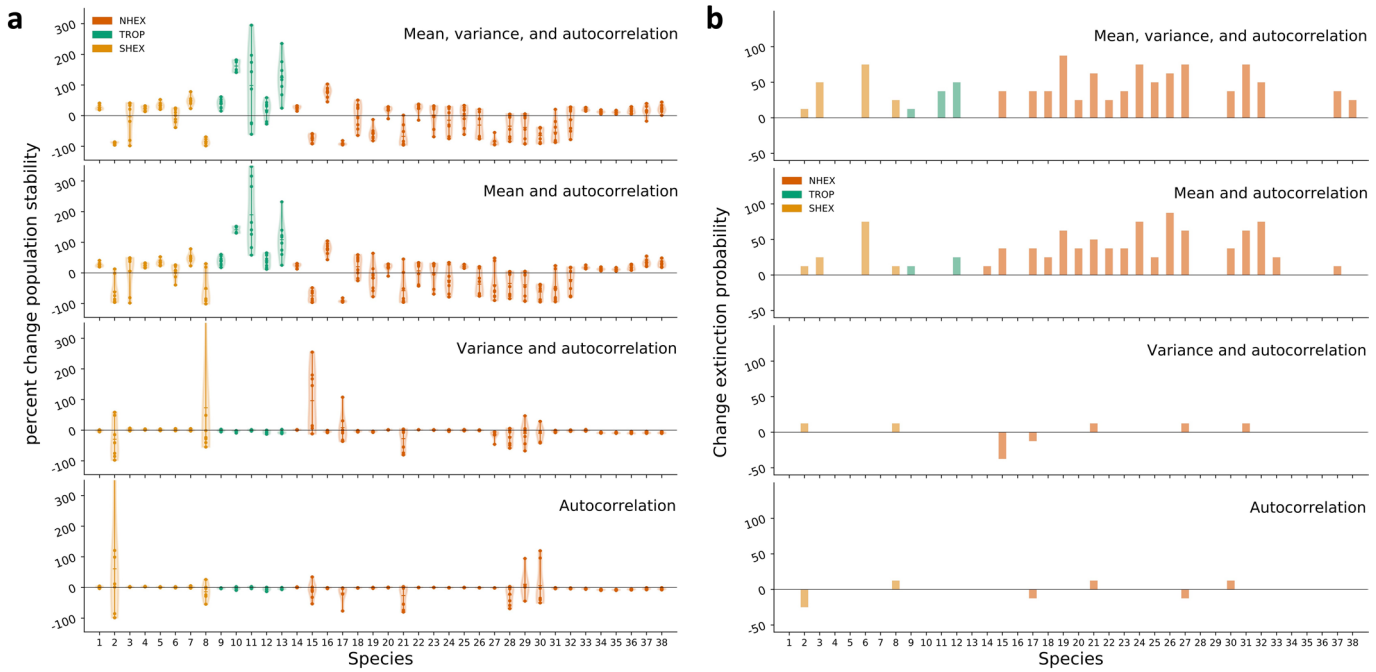

Extended Data Fig. 5 | Temperature-driven effects on population stability and extinction risk are robust to the degree of population self-regulation. Results exhibited limited sensitivity to strong ($\alpha = 1$; Fig. 4) and weak ($\alpha = 0.1$; above) self-regulation in the form of crowding effects. Latitudinal patterns and effect sizes were consistent for changes in population stability, **a**, and extinction probability, **b**.

https://doi.org/10.1038/s41558-022-01490-7

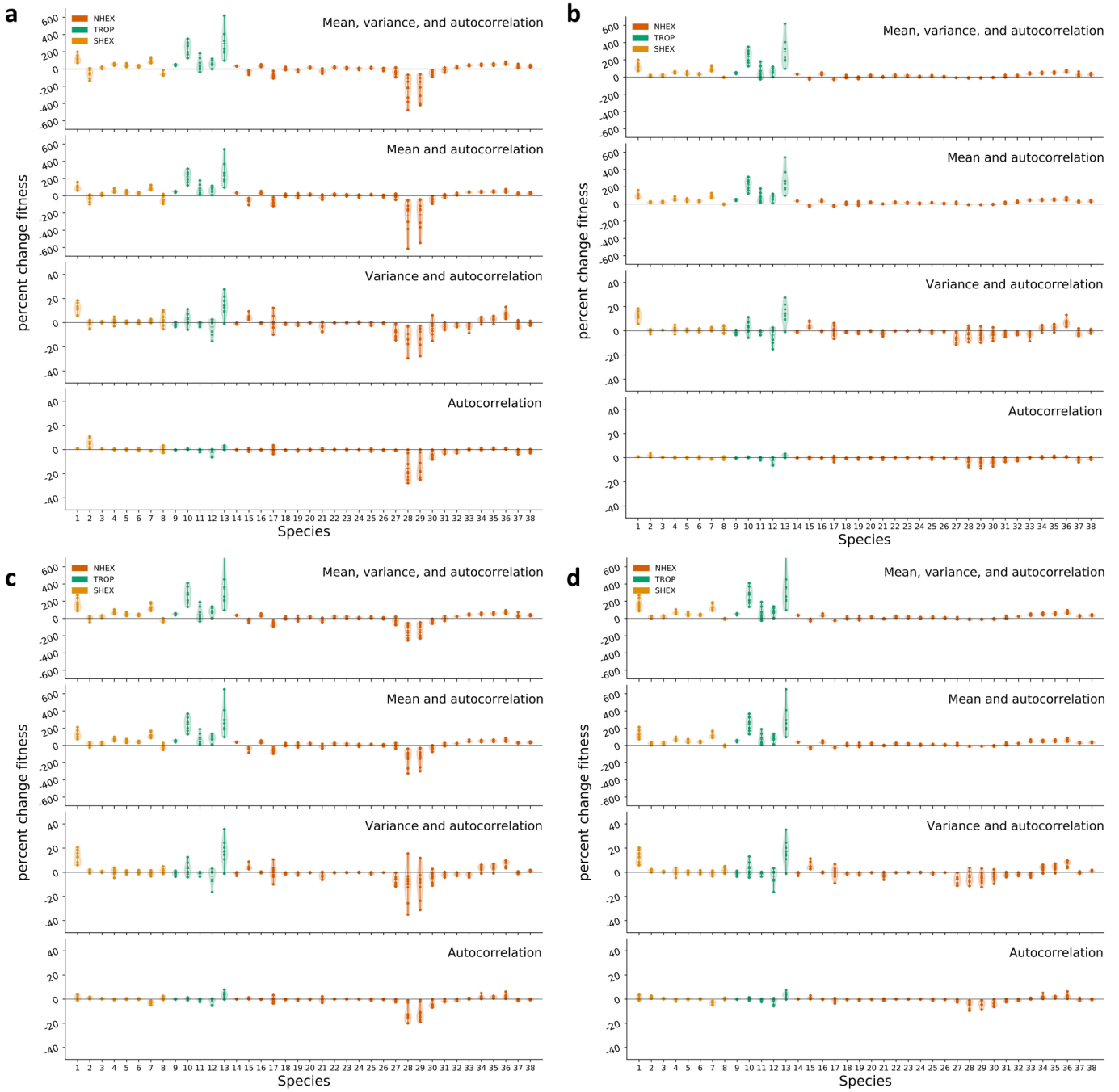

Extended Data Fig. 6 | Patterns of species risk are sensitive to treatment of high-temperature performance. Percent change in the average fitness (growth rate) driven by daily temperature between the historical period (1950-2000) and future period (2050-2100) when allowing negative growth rates above CTmax as in Vasseur et al. 2014 (**a**) and when performance values are bounded by 0 above CTmax as in Deutsch et al. 2008 (**b**). Percent change in the average fitness (growth rate) driven by monthly mean temperature between the historical period and future period when allowing negative growth rates above CTmax (**c**) and when performance values are bounded by 0 above CTmax (**d**).

https://doi.org/10.1038/s41558-022-01490-7

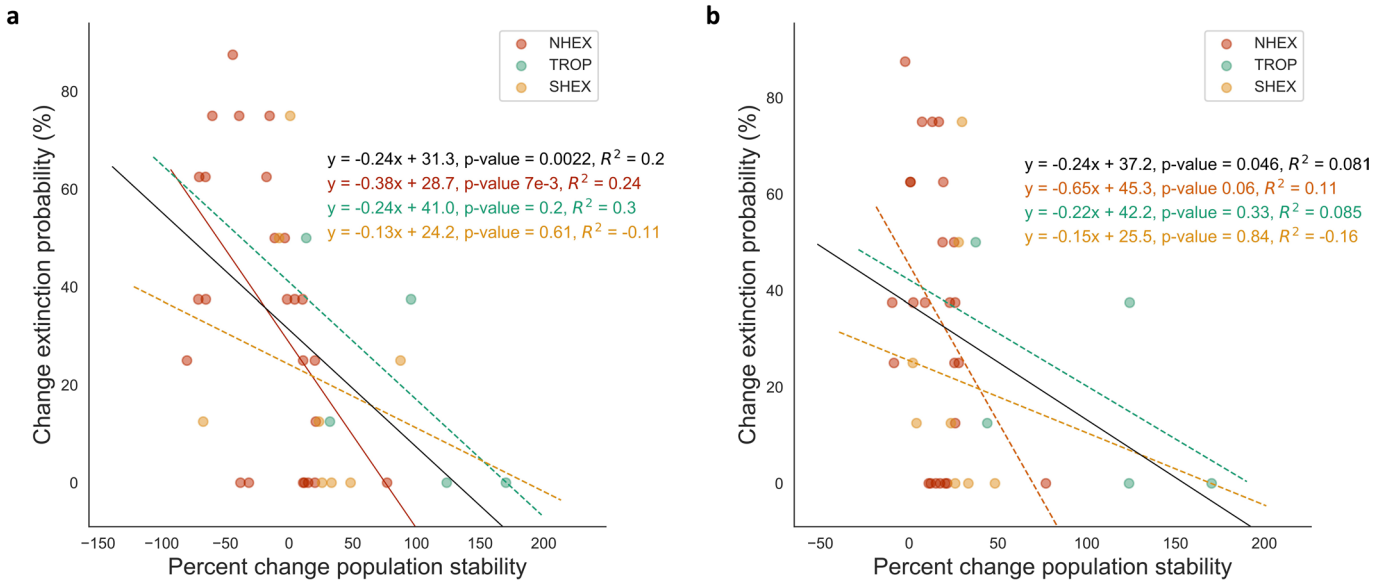

Extended Data Fig. 7 | Increased stability is negatively related to extinction probability. Regression relationships in our simulations are presented **a**, when considering only the pre-extinction time period and **b**, when taking into account the full 50-year periods. Regardless of largely positive (**b**) or mixed (**a**) changes in stability, there is generally a weak but significant negative relationship between stability and extinction probability globally (p-value < 0.05).

nature portfolio

Corresponding author(s): Kate Duffy

Last updated by author(s): Aug 23, 2022

Reporting Summary

Nature Portfolio wishes to improve the reproducibility of the work that we publish. This form provides structure for consistency and transparency in reporting. For further information on Nature Portfolio policies, see our Editorial Policies and the Editorial Policy Checklist.

Statistics

For all statistical analyses, confirm that the following items are present in the figure legend, table legend, main text, or Methods section.

n/a	Confirmed
☐	☒ The exact sample size (*n*) for each experimental group/condition, given as a discrete number and unit of measurement
☐	☒ A statement on whether measurements were taken from distinct samples or whether the same sample was measured repeatedly
☐	☒ The statistical test(s) used AND whether they are one- or two-sided *Only common tests should be described solely by name; describe more complex techniques in the Methods section.*
☐	☒ A description of all covariates tested
☐	☒ A description of any assumptions or corrections, such as tests of normality and adjustment for multiple comparisons
☐	☒ A full description of the statistical parameters including central tendency (e.g. means) or other basic estimates (e.g. regression coefficient) AND variation (e.g. standard deviation) or associated estimates of uncertainty (e.g. confidence intervals)
☐	☒ For null hypothesis testing, the test statistic (e.g. *F*, *t*, *r*) with confidence intervals, effect sizes, degrees of freedom and *P* value noted *Give P values as exact values whenever suitable.*
☒	☐ For Bayesian analysis, information on the choice of priors and Markov chain Monte Carlo settings
☒	☐ For hierarchical and complex designs, identification of the appropriate level for tests and full reporting of outcomes
☐	☒ Estimates of effect sizes (e.g. Cohen's *d*, Pearson's *r*), indicating how they were calculated

Our web collection on statistics for biologists contains articles on many of the points above.

Software and code

Policy information about availability of computer code

Data collection	No software was used for data collection in this study.
Data analysis	Open source codes were used to analyze the data, including R package quantreg v5.88 and R package biwavelet v0.02.21. Custom codes for analysis are available in our public GitHub repository at https://github.com/KateDuffy/climate-change-ecology

For manuscripts utilizing custom algorithms or software that are central to the research but not yet described in published literature, software must be made available to editors and reviewers. We strongly encourage code deposition in a community repository (e.g. GitHub). See the Nature Portfolio guidelines for submitting code & software for further information.

Data

Policy information about availability of data

All manuscripts must include a data availability statement. This statement should provide the following information, where applicable:

- Accession codes, unique identifiers, or web links for publicly available datasets
- A description of any restrictions on data availability
- For clinical datasets or third party data, please ensure that the statement adheres to our policy

The CMIP6 simulation data used in this paper is available via the data portal https://esgf-node.llnl.gov/search/cmip6/. The ecology data is available for download at https://doi.org/10.1073/pnas.0709472105.

Human research participants

Policy information about studies involving human research participants and Sex and Gender in Research.

Reporting on sex and gender	Not applicable
Population characteristics	Not applicable
Recruitment	Not applicable
Ethics oversight	Not applicable

Note that full information on the approval of the study protocol must also be provided in the manuscript.

Field-specific reporting

Please select the one below that is the best fit for your research. If you are not sure, read the appropriate sections before making your selection.

☐ Life sciences ☐ Behavioural & social sciences ☒ Ecological, evolutionary & environmental sciences

For a reference copy of the document with all sections, see nature.com/documents/nr-reporting-summary-flat.pdf

Ecological, evolutionary & environmental sciences study design

All studies must disclose on these points even when the disclosure is negative.

Study description	Using simulations from the latest generation of earth system models, we applied quantile, spectral, and wavelet analyses of temperature projections to study the way that temperatures will increase over time. We integrated temperature projections into empirically-parameterized mathematical models that simulate the dynamical and cumulative effects of thermal stress on the performance of 38 global ectotherm species.
Research sample	We obtained experimentally derived thermal tolerance parameters for a set of terrestrial ectotherms of the phylum arthropoda (n = 38) published by Deutsch et al. (2008). Deutsch gathered data from 31 previously published thermal performance studies, which were published between 1974 and 2003 based on a collection of insects from 35 different locations. For each species, experimental intrinsic growth rates at multiple temperatures were used to fit a thermal performance curve yielding least-squares estimates of the the curve's parameters. This dataset was selected to represent a globally distributed set of arthropod species.
Sampling strategy	Not applicable to study. We analyzed existing data as described in the data availability statement.
Data collection	Not applicable to study. We analyzed existing data as described in the data availability statement.
Timing and spatial scale	Not applicable to study. We analyzed existing data as described in the data availability statement.
Data exclusions	No data were excluded from the analysis.
Reproducibility	Our study consists of fully reproducible data analysis.
Randomization	Not applicable.
Blinding	Not relevant to study.

Did the study involve field work? ☐ Yes ☒ No

Reporting for specific materials, systems and methods

We require information from authors about some types of materials, experimental systems and methods used in many studies. Here, indicate whether each material, system or method listed is relevant to your study. If you are not sure if a list item applies to your research, read the appropriate section before selecting a response.

Materials & experimental systems

n/a	Involved in the study
☒	☐ Antibodies
☒	☐ Eukaryotic cell lines
☒	☐ Palaeontology and archaeology
☒	☐ Animals and other organisms
☒	☐ Clinical data
☒	☐ Dual use research of concern

Methods

n/a	Involved in the study
☒	☐ ChIP-seq
☒	☐ Flow cytometry
☒	☐ MRI-based neuroimaging